NJC

ROYAL SOCIETY OF CHEMISTRY

PAPER

View Article Online
View Journal | View Issue

Cite this: *New J. Chem.*, 2025, **49**, 5766

Cyclam-based molybdenum carbonyl complexes as a novel class of cytotoxic agents†

Tamara Teles,[abc] Auguste Fernandes,[b] Maria João Ferreira,[b] Leonor Côrte-Real,[b] Fernanda Marques,[c] João D. G. Correia *[c] and Luis G. Alves *[b]

Received 6th December 2024,
Accepted 4th March 2025

DOI: 10.1039/d4nj05233a

rsc.li/njc

Cyclam-based molybdenum carbonyl complexes of formulae [(H_2R_2Cyclam)Mo(CO)$_3$] (R = H, $^{4\text{-}t\text{Bu}}$PhCH$_2$, $^{4\text{-CF}3}$PhCH$_2$ and $^{3,5\text{-Me}}$PhCH$_2$) were prepared in high yields by the reaction of Mo(CO)$_6$ with the appropriate ligand precursor under reflux in di-*n*-butyl ether. All complexes were characterized by elemental analysis, IR, UV-Vis and NMR spectroscopy, thermogravimetry as well as single-crystal X-ray diffraction in the case of [(H_4Cyclam)Mo(CO)$_3$]. The cytotoxic effect of all compounds was examined on the human breast cancer cells MCF-7 and MDA-MB-231 revealing high antiproliferative activity.

Introduction

Cancer is currently one of the leading causes of mortality and an important barrier to life expectancy increase worldwide.[1,2] Chemotherapy is one of the most used treatments against cancer, either as the main approach or in combination with radiotherapy and/or surgery.[3] Platinum-based compounds are broadly used chemotherapeutic drugs but their inefficacy against drug-resistant tumours and severe side effects impelled the search for novel cytotoxic compounds, including novel metal-based drugs.[4] Within this context, several metal complexes have been studied as anticancer agents aiming to overcome resistance and the adverse effects of platinum-based drugs.[5] Rhenium,[6–9] ruthenium,[10–13] gold[14–17] and silver[18–21] complexes have been intensively studied due to their promising anticancer properties. Molybdenum compounds have gained much attention over the last years as novel metallodrugs for a wide range of therapeutic applications.[22] In particular, the activity of Na_2MoO_4,[23] polyoxomolybdates,[24,25] and Mo complexes[26–35] against various cancer cell lines disclosed their potential use as anticancer agents.

Late transition metal complexes of zinc,[36] cobalt,[37,38] ruthenium,[39] iron,[40] and copper[40–42] stabilized by cyclam derivatives have been studied as anticancer agents revealing moderate to good cytotoxic activities. Nevertheless, the research on early transition metal complexes based on cyclam derivatives as anticancer agents is limited to chromium complexes anchored on naphthalimide-cyclam conjugates.[36] In this work, we report the synthesis, characterization, and evaluation of the cytotoxic activity of cyclam-based Mo(0) carbonyl complexes against human breast cancer cells MCF-7 and MDA-MB-231. As far as we are aware, this class of compounds is the first molybdenum carbonyl complexes to be ever tested against breast cancer cells.

Results and discussion

Synthesis and characterization

Molybdenum complexes of the type [(H_2R_2Cyclam)Mo(CO)$_3$] (R = H, **5**; $^{4\text{-}t\text{Bu}}$PhCH$_2$, **6**; $^{4\text{-CF}3}$PhCH$_2$, **7** and $^{3,5\text{-Me}}$PhCH$_2$, **8**) were obtained in high yields by reaction of Mo(CO)$_6$ with the respective H_2R_2Cyclam derivative (R = H, **1**, $^{4\text{-}t\text{Bu}}$PhCH$_2$, **2**, $^{4\text{-CF}3}$PhCH$_2$, **3** and $^{3,5\text{-Me}}$PhCH$_2$, **4**) in refluxing di-*n*-butyl ether, as shown in Scheme 1. All complexes were characterized by elemental analysis, FT-IR, UV-Vis and ^{1}H/^{13}C-NMR spectroscopy, thermogravimetry as well as single-crystal X-ray diffraction in the case of complex **5**. Brought together the analytical data confirm the structure assigned to the complexes.

The IR spectra of complexes **5–8** (Fig. S1–S4, ESI†) show very weak bands in the range 3300–3000 cm^{-1} assigned to the stretching vibrational ν_{N-H} modes of the free and H-bonded N–H groups of the cyclam rings. The δ_{N-H} vibrational modes might be also observed at lower frequencies but are probably overlapped with other vibrational bands (*e.g.* ν_{C-H}, vibrations at 1450–1300 cm^{-1}). The vibrational bands assigned to the C–F bonds stretching of –CF$_3$ groups in **7** appear at 1124 and

[a] *NOVA School of Science and Technology/FCT-NOVA, Campus de Caparica, 2829-516 Caparica, Portugal*
[b] *Centro de Química Estrutural – Institute of Molecular Sciences, Associação do Instituto Superior Técnico para a Investigação e Desenvolvimento, Av. António José de Almeida 12, 1000-043 Lisboa, Portugal. E-mail: luis.g.alves@tecnico.ulisboa.pt*
[c] *Centro de Ciências e Tecnologias Nucleares and Departamento de Engenharia e Ciências Nucleares, Instituto Superior Técnico, Universidade de Lisboa, CTN, Estrada Nacional 10 (km 139,7), 2695 – 066 Bobadela LRS, Portugal. E-mail: jgalamba@ctn.tecnico.ulisboa.pt*

† Electronic supplementary information (ESI) available: Supplementary figures and tables. CCDC 2301353. For ESI and crystallographic data in CIF or other electronic format see DOI: https://doi.org/10.1039/d4nj05233a

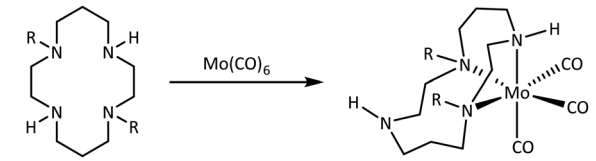

R = H 1
R = 4-tBuPhCH2 2
R = 4-CF3PhCH2 3
R = 3,5-MePhCH2 4

R = H 5
R = 4-tBuPhCH2 6
R = 4-CF3PhCH2 7
R = 3,5-MePhCH2 8

Scheme 1 Synthetic route for the preparation of complexes **5–8**.

1063 cm^{-1} revealing a slightly shift to higher frequencies when compared to those observed for the ligand precursor **3** (1105 and 1064 cm^{-1}).[43] The characteristic carbonyl stretching bands at 1892, 1765 and 1732 cm^{-1} in **6**, 1889 and 1735 cm^{-1} in **7** and 1885 and 1735 cm^{-1} in **8** are in the same range of those reported for **5** (1896 and 1740 cm^{-1}) and thus, consistent with *fac*-[LM(CO)$_3$] species.[44] This suggestion is also in line with the molecular structure of **5** obtained by single crystal X-ray diffraction detailed below (Fig. 1).

The UV-visible absorption spectra of complexes **5–8** were recorded in DMSO (Fig. S5, ESI†). The spectra show one intense absorption band around 319 nm attributed to metal–ligand charge transfer (MLCT).[45] Compound **5** also shows a low intense band around 455 nm, which may be ascribed as a d–d transition (Laporte forbidden). This band is not observed in the other complexes, possibly due to the influence of the benzylic arms of the cyclam ring of ligands **2–4**, which may enhance the ligand field strength around the metal centre. This may result in an increased octahedral crystal field splitting energy, shifting the d–d transitions to higher energy. The transition bands from the ligands ($\pi \rightarrow \pi^*$ and $n \rightarrow \pi^*$ for CO and $n \rightarrow \sigma^*$ for cyclam) appear below the solvent cut-off (<280 nm).

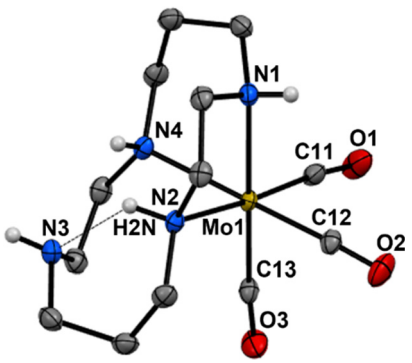

Fig. 1 ORTEP depiction of the solid-state molecular structure of **5** showing thermal ellipsoids at 40% probability level. Selected hydrogen atoms and co-crystallized dichloromethane were omitted for clarity. Hydrogen bonds are represented as dashed lines. Selected bond lengths (Å) and angles (°): Mo(1)–N(1) 2.321(2), Mo(1)–N(2) 2.334(2), Mo(1)–N(4) 2.359(2), Mo(1)–C(11) 1.929(3), Mo(1)–C(12) 1.924(3), Mo(1)–C(13) 1.936(3); N(1)–Mo(1)–C(13) 179.1(1), N(2)–Mo(1)–C(11) 173.4(1), N(4)–Mo(1)–C(12) 174.7(1).

The ^{1}H NMR spectrum of **5** shows four broad signals integrating to one proton each at 5.01, 4.73, 2.16 and 1.83 ppm corresponding to the NH protons and as expected, only two resonances attributed to this type of protons are observed in complexes **5–8**. The two AB systems observed in the spectra of **6–8** due to the PhCH_2N protons ($^3J_{H-H}$ = 12–15 Hz) are indicative of the coordination of the two *N*-benzyl nitrogen atoms to the metal centre. The methylene protons belonging to the cyclam ring in complexes **4–8** appear as twenty multiplets integrating to one proton each. The $^{13}C\{^1H\}$ NMR spectra of **4–8** reveal ten resonances attributed to the macrocyclic backbone and the benzylic carbons of the pendant arms of the macrocycle give raise to two resonances. The carbon resonances due to the CO ligands appear as three signals at 228.9, 228.5 and 227.7 ppm in **5** and at 229.4, 227.8 and 227.6 ppm in **6**. Owing to the poor solubility of compounds **7** and **8**, resonances due to CO and CF_3 groups could not be observed in solution but they were identified by solid-state ^{13}C CP MAS NMR. The proton and carbon resonances patterns observed for complexes **5–8** are consistent with a C_1 symmetry, which is maintained both in solution (Fig. S6–S9, ESI†) and in the solid-state (Fig. S10 and S11, ESI†).

Thermogravimetric analyses of complexes **5–8** (Fig. S12–S15, ESI†) show thermal decomposition in two stages. The first stage corresponds to the loss of two carbonyl ligands that occurs below 200 °C for all compounds. The last stage proceeded with two degradation steps in **5** and various steps in **6–8** that correspond to the loss of the macrocycle and the remaining carbonyl ligand. The overall weight loss is completed below 650 °C leaving a metallic Mo residue. TG-DSC data for complexes **5–8** are summarized in Table S1 (ESI†).

Complex **5** crystallized in the monoclinic space group $P2_1/n$ with one molecule of dichloromethane in the asymmetric unit. Crystallographic and experimental details of data collection and crystal structure determinations are presented in Table S2 (ESI†). The solid-state molecular structure depicted in Fig. 1 reveals a distorted octahedral geometry with two nitrogen atoms of the macrocycle (N(2) and N(4)) and two carbonyl ligands occupying a slightly twisted square plane with combined equatorial angles of 359.7°. The axial positions are occupied by the nitrogen atom N(1) and the other carbonyl ligand displaying a N(1)–Mo(1)–C(13) angle of 179.1(1)°. An intramolecular hydrogen bond established by N(2)–H(2)···N(3) is observed with a distance of 2.20 Å forming a six-membered heterocycle. The overall bond distances and angles determined for **5** are in agreement with values reported for other Mo(0) carbonyl complexes supported by tetraazamacrocycles.[44,46]

Stability assays

The UV-visible spectra of complexes **5–8** recorded in DMEM supplemented with 10% FBS (Fig. S16–S19, ESI†) are similar to those recorded in DMSO revealing no bathochromic or hypsochromic shifts. However, a decrease on the absorbance over time is observed for all complexes that might be related to a decline in their solubility in line with the formation of white precipitates. This effect is more pronounced in complex **5** that

reveals total precipitation out of solution after 24 h, which may explain its poor antitumoral activity (see discussion bellow). The ^{1}H NMR spectra recorded from DMSO solutions of **5–8** show no significant changes after 6 days (Fig. S20–S23, ESI†). This result validates the stability of the compounds in solution and points out that precipitates formed in DMEM with 10% FBS might be due to the formation of aggregates between compounds and proteins present in the medium rather than decomposition suggesting that complexes are stable for 72 h (cytotoxic assays time).

Cytotoxic assays

The cytotoxic activity of compounds **1–8** was determined against the human breast cancer cells MCF-7 (hormone dependent, estrogen receptor (ER) and progesterone receptor (PR) positives and HER-2 oncogene negative) and MDA-MB-231 (triple negative (TNBC), ER, PR and HER-2 negatives) as well as on the normal human dermal fibroblasts (HDF). Cells were incubated with each compound (complexes and ligand precursors) continuously for 72 h and then assayed for cellular viability using the MTT assay. The IC_{50} values for the cellular viability are summarized in Table 1. The results show that cyclam, **1**, display no cytotoxic activity against both cancer cells (MCF-7 and MDA-MB-231) but the ligand precursors **2–4** display high activity against both cancer cells and normal fibroblasts. Furthermore, compound **2** is highly active against the TNBC cells MDA-MB-231. Complex **5** is the less active complex but reveals high selectivity for MCF-7 cells. Complexes **6–8** display similar anticancer activity against the MCF-7 cells when compared to the corresponding ligand precursors **2–4** but they are less cytotoxic to the normal fibroblasts that show high selectivity for the breast cancer cells MCF-7. Remarkably, both ligand precursors **2–4** and complexes **6–8** show a better performance than cisplatin in the same experimental conditions.[47,48]

The selectivity index (SI) of compounds **2–8** based on the ratio IC_{50} in fibroblasts/IC_{50} in a cancer cell line, was determined to evaluate the selectivity of each compound towards cancer cells. The results show that a favorable SI $\geq$ 3 was found for **7** and **8** with the MCF-7 cells suggesting that these complexes could be considered prospective anticancer drugs to be further explored against this type of human breast cancer model.[49]

Table 1 IC_{50} values obtained for compounds **1–8** against breast cancer cell lines (MCF-7 and MDA-MB-231) and normal fibroblasts (HDF) after 72 h

	IC_{50} (μM)			
	MCF-7	MDA-MB-231	HDF	SI[a]
1	$\gg$100	$\gg$100	—	—
2	2.3 ± 1.9	0.8 ± 0.3	2.9 ± 1.9	1.3/3.6
3	2.6 ± 1.5	2.7 ± 1.6	2.9 ± 1.7	1.1/1.1
4	3.0 ± 2.6	1.7 ± 0.7	4.4 ± 1.7	1.5/2.6
5	42.6 ± 16.0	$\gg$100	$\gg$100	>2.3/–
6	2.3 ± 1.2	1.6 ± 0.7	2.9 ± 1.1	1.3/1.8
7	2.9 ± 1.9	6.8 ± 3.2	15.8 ± 13.2	5.4/2.3
8	1.8 ± 1.0	21.5 ± 6.4	11.6 ± 3.8	6.4/0.5
cisplatin	26.7 ± 1.7[47]	16.3 ± 2.3[47]	6.3 ± 1.8[48]	0.2/0.4

[a] The SI (selectivity index) was calculated using the formula: SI = (IC_{50} for normal fibroblasts/IC_{50} for breast cancer cells). SI value $\geq$ 3 indicates a prospective anticancer agent.[49]

Experimental

General considerations

Ligand precursors **1–4**[50,51] and complex **5**[44] were prepared according to previously published procedures. $Mo(CO)_6$ was purchased from Sigma-Aldrich and purified by sublimation. Di-*n*-butyl ether and diethyl ether were refluxed over sodium-benzophenone and collected by distillation. Dichloromethane was refluxed over calcium hydride and collected by distillation. All other reagents were commercial grade and used without purification. Deuterated dimethylsulfoxide (DMSO-d_6) was dried with 4 Å molecular sieves and freeze–pump–thaw degassed prior to use. All manipulations were performed under an atmosphere of dry oxygen-free nitrogen by means of standard Schlenk and glovebox techniques.

Synthetic procedures

[(H_4Cyclam)Mo(CO)$_3$], 5. A mixture of $Mo(CO)_6$ (0.48 g, 1.82 mmol) and 1,4,8,11-tetraazacyclotetradecane, **1** (0.36 g, 1.80 mmol) was refluxed in di-*n*-butyl ether for 3 h. The reaction mixture was allowed to cool to room temperature, filtered, and the precipitate was washed with di-*n*-butyl ether, and dried in vacuum to give compound **5** as a brown solid (0.53 g, 76%). Crystaline material suitable for single-crystal X-ray diffraction were obtained from a concentrated dichloromethane solution at −80 °C. ^{1}H NMR (DMSO-d_6, 400.1 MHz, 296 K): δ (ppm) 5.01 (br, 1H, NH), 4.73 (br, 1H, NH), 3.69 (m, 1H, CH_2N), 3.07–2.96 (overlapping, 2H total, CH_2N), 2.82–2.56 (overlapping, 12H total, 11H, CH_2N and 1H, $CH_2CH_2CH_2$), 2.40–2.34 (overlapping, 2H total, CH_2N), 2.16 (br, 1H, NH), 2.00 (m, 1H, $CH_2CH_2CH_2$), 1.83 (br, 1H, NH), 1.57 (m, 1H, $CH_2CH_2CH_2$), 1.31 (m, 1H, $CH_2CH_2CH_2$). $^{13}C\{^1H\}$ NMR (DMSO-d_6, 100.6 MHz, 296 K): δ (ppm) 228.9 (CO), 228.5 (CO), 227.7 (CO), 56.8 (CH_2N), 55.5 (CH_2N), 55.3 (CH_2N), 53.5 (CH_2N), 50.4 (CH_2N), 48.1 (CH_2N), 44.7 (CH_2N), 43.2 (CH_2N), 24.2 ($CH_2CH_2CH_2$), 23.9 ($CH_2CH_2CH_2$). FT-IR (ATR, cm^{-1}): 1896 ($\nu_{C\equiv O}$), 1740 ($\nu_{C\equiv O}$). UV-vis (DMSO) λ_{max}, nm: 319 (ε = 3384 M^{-1} cm^{-1}), 455 (ε = 179 M^{-1} cm^{-1}). Anal. calcd for $C_{13}H_{24}MoN_4O_3.(CH_2Cl_2)_{0.5}$: C, 38.35; H, 5.96; N, 13.25. Found: C, 38.26; H, 5.80; N, 14.43.

[{H_2(4-^{t}BuPhCH$_2$)$_2$Cyclam}Mo(CO)$_3$], 6. A mixture of $Mo(CO)_6$ (0.13 g, 0.51 mmol) and 1,8-bis(4-(*tert*-butyl)benzyl)-1,4,8,11-tetraazacyclotetradecane, **3** (0.25 g, 0.51 mmol) was refluxed in a di-*n*-butyl ether/diethyl ether mixture (2 : 1) for 3 h. The reaction mixture was allowed to cool to room temperature, filtered, and the precipitate was washed with diethyl ether, and dried in vacuum to give compound **6** as an off-white solid (0.25 g, 72%). ^{1}H NMR (DMSO-d_6, 400.1 MHz, 296 K): δ (ppm) 7.36 (d, $^3J_{H-H}$ = 8 Hz, 2H, $PhCH_2N$), 7.34 (d, $^3J_{H-H}$ = 9 Hz, 2H, $PhCH_2N$), 7.20 (d, $^3J_{H-H}$ = 8 Hz, 2H, $PhCH_2N$), 7.18 (d, $^3J_{H-H}$ = 9 Hz, 2H, $PhCH_2N$), 4.62 (br, 1H, NH), 4.53 (d, 1H, $^3J_{H-H}$ = 14 Hz, $PhCH_2N$), 4.18 (d, 1H, $^3J_{H-H}$ = 14 Hz, $PhCH_2N$), 3.99 (m, 1H, CH_2N), 3.51 (d, 1H, $^3J_{H-H}$ = 13 Hz, PhCH_2N), 3.44 (d, 1H, $^3J_{H-H}$ = 13 Hz, $PhCH_2N$), 3.10–2.98 (overlapping, 2H, CH_2N), 2.95–2.78 (overlapping, 5H total, CH_2N), 2.59–2.55 (overlapping, 3H, CH_2N), 2.38–2.34 (overlapping, 2H total, CH_2N), 2.18–2.10 (overlapping, 3H total, CH_2N), 1.55–1.46

(overlapping, 4H total, $CH_2CH_2CH_2$), 1.25 (s, 9H, $C(CH_3)_3$), 1.17 (s, 9H, $C(CH_3)_3$), 0.83 (m, 1H, NH). $^{13}C\{^1H\}$ NMR (DMSO-d_6, 100.6 MHz, 296 K): δ (ppm) 229.4 (CO), 227.8 (CO), 227.6 (CO), 150.5 (i-$PhCH_2N$), 150.0 (i-$PhCH_2N$), 136.1 (*p*-$PhCH_2N$), 132.3 ($PhCH_2N$), 128.6 ($PhCH_2N$), 128.3 (*p*-$PhCH_2N$), 125.4 ($PhCH_2N$), 124.8 ($PhCH_2N$), 65.1 ($PhCH_2N$), 60.8 ($PhCH_2N$), 57.1 (CH_2N), 56.8 (CH_2N), 56.3 (CH_2N), 54.6 (CH_2N), 54.3 (CH_2N), 50.5 (CH_2N), 49.9 (CH_2N), 46.1 (CH_2N), 34.3 ($C(CH_3)_3$), 34.2 ($C(CH_3)_3$), 31.0 (overlapping, 2 × $C(CH_3)_3$), 25.1 ($CH_2CH_2CH_2$), 24.4 ($CH_2CH_2CH_2$). FT-IR (ATR, cm^{-1}): 1892 ($\nu_{C\equiv O}$), 1765 ($\nu_{C\equiv O}$), 1732 ($\nu_{C\equiv O}$). UV-vis (DMSO) λ_{max}, nm: 320 (ε = 3018 M^{-1} cm^{-1}). Anal. calcd for $C_{35}H_{52}MoN_4O_3$: C, 62.48; H, 7.79; N, 8.33. Found: C, 62.69; H, 7.68; N, 8.23.

[{H$_2$(4-CF$_3$PhCH$_2$)$_2$Cyclam}Mo(CO)$_3$], 7. A mixture of $Mo(CO)_6$ (0.50 g, 1.89 mmol) and 1,8-bis(4-(trifluoromethyl)benzyl)-1,4,8,11-tetraazacyclotetradecane, **3** (0.98 g, 1.90 mmol) was refluxed in di-*n*-butyl ether for 3 h. The reaction mixture was allowed to cool to room temperature, filtered, and the precipitate was washed with di-*n*-butyl ether, and dried in vacuum to give compound **7** as an off-white solid (1.23 g, 93%). ^1H NMR (DMSO-d_6, 300.1 MHz, 296 K): δ (ppm) 7.73–7.70 (overlapping, 4H total, *Ph*CH_2N), 7.56 (d, $^3J_{H-H}$ = 8 Hz, 2H, $PhCH_2N$), 7.48 (d, $^3J_{H-H}$ = 7 Hz, 2H, $PhCH_2N$), 4.69–4.59 (overlapping, 2H total, 1H, NH, 1H, $^3J_{H-H}$ = 13 Hz, $PhCH_2N$), 4.35 (d, $^3J_{H-H}$ = 15 Hz, 1H, $PhCH_2N$), 4.09–4.03 (overlapping, 2H, CH_2N), 3.81 (d, $^3J_{H-H}$ = 15 Hz, 1H, $PhCH_2N$), 3.41 (d, $^3J_{H-H}$ = 13 Hz, 1H, $PhCH_2N$), 3.18–3.03 (overlapping, 3H total, 1H, CH_2N), 2.87–2.84 (overlapping, 3H total, CH_2N), 2.73–2.69 (overlapping, 3H total, CH_2N), 2.45–2.36 (overlapping, 5H total, CH_2N), 1.72–1.67 (overlapping, 2H total, $CH_2CH_2CH_2$), 1.45–1.42 (overlapping, 2H total, $CH_2CH_2CH_2$), 0.83 (m, 1H, NH). $^{13}C\{^1H\}$ NMR (DMSO-d_6, 75.5 MHz, 296 K): δ (ppm) 143.3 (i-$PhCH_2N$), 135.8 (i-*Ph*CH_2N), 133.5 (*o*-$PhCH_2N$), 130.0 (*o*-$PhCH_2N$), 125.4 (q, $^3J_{C-F}$ = 4 Hz, *m*-$PhCH_2N$), 124.8 (q, $^3J_{C-F}$ = 4 Hz, *m*-$PhCH_2N$), 64.6 ($PhCH_2N$), 59.1 ($PhCH_2N$), 56.7 (CH_2N), 56.5 (CH_2N), 55.7 (CH_2N), 54.7 (CH_2N), 53.6 (CH_2N), 49.9 (overlapping, 2xCH_2N), 46.3 (CH_2N), 24.7 ($CH_2CH_2CH_2$), 24.3 ($CH_2CH_2CH_2$). ^{19}F NMR (DMSO-d_6, 282.6 MHz, 296 K): δ (ppm) −60.9 (s, CF_3), −61.1 (s, CF_3). ^{13}C CP MAS NMR (500 MHz, 296 K): δ (ppm) 174.2 (CO or CF_3), 172.3 (CO or CF_3), 169.8 (CO or CF_3), 164.7 (CO or CF_3), 146.1 ($PhCH_2N$), 134.8 ($PhCH_2N$), 132.6 ($PhCH_2N$), 130.1 ($PhCH_2N$), 126.9 ($PhCH_2N$), 125.1($PhCH_2N$), 64.6 ($PhCH_2N$ or CH_2N), 60.7 ($PhCH_2N$ or CH_2N), 59.0 ($PhCH_2N$ or CH_2N), 58.0 ($PhCH_2N$ or CH_2N), 55.1 (CH_2N), 53.1 (CH_2N), 51.9 (CH_2N), 49.9 (CH_2N), 47.7 (CH_2N), 45.8 (CH_2N), 24.8 ($CH_2CH_2CH_2$), 22.4 (CH_2-CH_2CH_2). FT-IR (ATR, cm^{-1}): 1889 ($\nu_{C\equiv O}$), 1735 ($\nu_{C\equiv O}$), 1124 (ν_{C-F}), 1063 (ν_{C-F}). UV-vis (DMSO) λ_{max}, nm: 319 (ε = 2732 M^{-1} cm^{-1}). Anal. calcd for $C_{29}H_{34}F_6MoN_4O_3$: C, 50.01; H, 4.92; N, 8.04. Found: C, 49.79; H, 4.91; N, 8.03.

[{H$_2$(3,5-Me PhCH$_2$)$_2$Cyclam}Mo(CO)$_3$], 8. A mixture of $Mo(CO)_6$ (0.15 g, 0.57 mmol) and 1,8-bis(3,5-dimethylbenzyl)-1,4,8,11-tetraazacyclotetradecane, **4** (0.25 g, 0.57 mmol) was refluxed in di-*n*-butyl ether for 3 h. The reaction mixture was allowed to cool to room temperature, filtered, and the precipitate was washed with di-*n*-butyl ether, and dried in vacuum to give compound **8** as an off-white solid (0.24 g, 68%). ^1H NMR (DMSO-d_6, 400.1 MHz, 296 K): δ (ppm) 6.95–6.84 (overlapping, 6H, $PhCH_2N$), 4.60 (br, 1H, NH), 4.48 (d, 1H, $^3J_{H-H}$ = 12 Hz, $PhCH_2N$), 4.17 (d, $^3J_{H-H}$ = 12 Hz, 1H, $PhCH_2N$), 4.02 (m, 1H, CH_2N), 3.52 (d, 1H, $^3J_{H-H}$ = 12 Hz, $PhCH_2N$), 3.31 (d, 1H, $^3J_{H-H}$ = 12 Hz, $PhCH_2N$), 3.08–2.17 (overlapping, 27H total, 15H, CH_2N and 12H, CH_3), 1.66 (m, 2H, $CH_2CH_2CH_2$), 1.46 (m, 2H, $CH_2CH_2CH_2$), 1.20 (br, 1H, NH). $^{13}C\{^1H\}$ NMR (DMSO-d_6, 100.6 MHz, 296 K): δ (ppm) 130.9 (*o*-$PhCH_2N$), 130.0 (*p*-$PhCH_2N$), 127.7 (*p*-$PhCH_2N$), 127.1 (*o*-$PhCH_2N$), 66.3 ($PhCH_2N$), 60.8 ($PhCH_2N$), 57.3 (overlapping, 3 × CH_2N), 55.2 (CH_2N), 54.2 (CH_2N), 50.6 (overlapping, 2 × CH_2N), 46.1 (CH_2N), 25.5 ($CH_2CH_2CH_2$), 24.7 ($CH_2CH_2CH_2$), 21.4 (CH_3). ^{13}C CP MAS NMR (500 MHz, 296 K): δ (ppm) 178.9 (CO), 170.6 (CO), 140.4 ($PhCH_2N$), 139.2 ($PhCH_2N$), 138.0 ($PhCH_2N$), 137.5 ($PhCH_2N$), 131.6 ($PhCH_2N$), 131.0 ($PhCH_2N$), 129.9 ($PhCH_2N$), 126.3 ($PhCH_2N$), 68.7 (Ph*C*H_2N), 64.6 ($PhCH_2N$), 58.9 (CH_2N), 57.9 (overlapping, 2 × CH_2N), 57.2 (CH_2N), 55.9 (CH_2N), 51.9 (CH_2N), 50.4 (CH_2N), 47.9 (CH_2N), 27.1 ($CH_2CH_2CH_2$ or CH_3), 26.1 ($CH_2CH_2CH_2$ or CH_3), 23.5 ($CH_2CH_2CH_2$ or CH_3), 22.4 ($CH_2CH_2CH_2$ or CH_3), 21.3 ($CH_2CH_2CH_2$ or CH_3), 20.7 ($CH_2CH_2CH_2$ or CH_3). FT-IR (ATR, cm^{-1}): 1885 ($\nu_{C\equiv O}$), 1735 ($\nu_{C\equiv O}$). UV-vis (DMSO) λ_{max}, nm: 318 (ε = 3648 M^{-1} cm^{-1}). Anal. calcd for $C_{31}H_{44}MoN_4O_3$: C, 60.38; H, 7.19; N, 9.09. Found: C, 59.29; H, 7.88; N, 9.01.

Nuclear magnetic resonance spectroscopy

Solution NMR spectra were recorded in a Bruker AVANCE II 300 or 400 spectrometers, at 296 K, referenced internally to residual proton-solvent (^1H) or solvent (^{13}C) resonances, and reported relative to tetramethylsilane (0 ppm). 2D NMR experiments such as ^1H–^{13}C HSQC and ^1H–^1H COSY were performed in order to make all the assignments.

Solid-state NMR spectra were recorded in a Bruker AVANCE III 500 spectrometer, operating at B_0 field of 11.7 T, with ^1H and ^{13}C Larmor frequencies of 500.1 and 125.8 MHz, respectively. All experiments were performed in a 4 mm double-resonance MAS probe (Bruker) at 296 K. Samples were packed into a ZrO_2 rotor with Kel-F caps and spinned at 5 KHz. Spectra were referenced externally to TMS (for ^1H, 0 ppm) and glycine (for ^{13}C, CO at 176.03 ppm). The ^{13}C CP MAS spectra were acquired using the TOSS sequence to suppress spinning sidebands,[52] using phase cycling as described in the literature.[53] The following conditions were used: the ^1H 90° pulse was set to 2.5 μs corresponding to a radio frequence of ∼100 kHz. The CP step was performed with a contact time (CT) of 2000 μs using a 50–100% RAMP shape at the ^1H channel and using a 50 kHz square shape pulse on the ^{13}C channel; RD was 5 s. During the acquisition, a SPINAL-64 decoupling scheme was employed using a pulse length for the basic decoupling units of 5 μs at radio frequence field strength of 100 kHz.

Fourier-transform infrared spectroscopy

Fourier-transform infrared spectra were acquired with a Thermo Scientific Nicolet 6700 spectrometer, equipped with a single reflection smart miracle ATR accessory (ZnS crystal,

Pike Technology). Spectra were collected in the range 4000–650 cm^{-1} with 64 scans and a resolution of 4 cm^{-1}.

Thermogravimetric analysis

Thermogravimetric analyses were performed between 25 and 800 °C, using a Setsys Evo16 TG-DSC thermobalance (SETARAM), under air flow of 30 $cm^3.min^{-1}$ and with a heating rate of 10 °C min^{-1}.

Elemental analysis

Elemental analyses (C, H, N) were performed in a Fisons CHNS/O analyser Carlo Erba Instruments EA-1108 equipment at the Laboratório de Análises do Instituto Superior Técnico.

Single-crystal X-ray diffraction

Suitable crystals of compound **5** were coated and selected in Fomblin® oil under an inert atmosphere of nitrogen. Crystals were then mounted on a loop external to the glovebox environment and data collected using graphite-monochromated Mo-Kα radiation (λ = 0.71073 Å) on a Bruker AXS-KAPPA APEX II diffractometer (Bruker AXS Inc., Madison, WI, USA) equipped with an Oxford Cryosystem open-flow nitrogen cryostat. Data were corrected for Lorentzian polarization and absorption effects using SAINT[54] and SADABS[55] programs. The structure was solved by a direct method using SIR97.[56] Structure refinement was done using SHELXL-2018/3.[57] These programs are part of the WinGX-Version 2021.3 program package.[58] A full-matrix least-squares refinement was used for the non-hydrogen atoms with anisotropic thermal parameters. Hydrogen atoms of the NH groups were located in the electron density map. The other hydrogen atoms were inserted in idealized positions and allowed to refine in the parent carbon atoms. The illustration of the molecular structure of **5** was made with MERCURY 2022.3.0.[59] Data for structure **5** was deposited in the Cambridge Crystallographic Data Centre (CCDC) under the deposit number 2301353.

Ultraviolet-visible spectroscopy

UV-visible spectra were recorded from DMSO solutions with a Cary 60 UV-vis (Agilent Technologies) in the range of 280–800 nm.

Stability studies

Stock solutions of complexes **5–8** were freshly prepared in DMSO and diluted with complete Dulbecco's Modified Eagle Medium (DMEM) without phenol red (supplemented with 10% FBS) achieving a final concentration of 10^{-4} M (except for **5** that was 2×10^{-4} M), ensuring that the organic solvent content was less than 1% (v/v). UV-visible spectra were recorded over a set of time intervals (0, 4, 24, 48 and 72 h) on a Cary 60 UV-vis spectrophotometer (Agilent Technologies) using a quartz cuvette with 1 cm path length in a wavelength range of 280–800 nm.

Cell culture

Human breast cancer MCF-7 (ATCC, HTB-22) (hormone dependent, estrogen receptor (ER) and progesterone receptor (PR) positives and HER-2 oncogene negative) and MDA-MB-231 (ATCC, HTB-26) (triple negative, ER, PR and HER-2 negatives) cells were cultured in T25 cell culture flask containing DMEM supplemented with 10% FBS and 1% penicillin–streptomycin. Human dermal fibroblasts (HDF) were cultured in T25 cell culture flask containing Fibroblast Growth Medium (FGM, 116-500, Sigma-Aldrich). The cancer cells (MCF-7 and MDA-MB-231) and normal healthy cells (HDF) were grown in standard conditions, *i.e.*, incubated at 37 °C in a 5% CO_2 atmosphere in a humidified atmosphere. The culture medium was substituted whenever necessary (according to cell growth rate), both cancer and healthy cells were passed at approximately 80–90% confluency and used for further investigations.

Cytotoxic assays

Compounds were solubilized in DMSO and subsequently diluted in DMEM assuring that no more than 1% (v/v) of DMSO is present in the cell culture medium. Cells were collected after trypsinization followed by the quantification of cell viability, using the trypan blue exclusion method, where one part of trypan blue (about 20 μL) and one part cell suspension (about 20 μL) were mixed. Viable (unstained) and non-viable (stained) cells were counted in a hemocytometer using an inverted phase contrast microscope. Cells were plated into 96-well plates at *ca.* 1.5×10^4 cells per well density and incubated for 24 h in standard conditions before the addition of compounds **1–8** in a concentration range of 0.01–100 μM. After 72 h, culture medium was removed and a solution of 3-(4,5-dimethylthiazol-2-yl)-2,5-diphenyltetrazolium bromide (MTT) in phosphate buffered saline (PBS) was added to each well (about 200 μL). After 3 h of incubation at 37 °C in a 5% CO_2 atmosphere, the MTT solution was removed, and formazan crystals were solubilized in DMSO. Absorbance of the solution was read at 570 nm in a microplate reader (BioTek PowerWave XS). The half maximal inhibitory concentration (IC_{50}) values were determined using the 9.0 GraphPad Prism software and the obtained data refer to four replicates for each concentration.

Conclusions

Cyclam-based molybdenum carbonyl complexes of formulae $[(H_2R_2Cyclam)Mo(CO)_3]$ (R = H, $^{4\text{-}t\text{Bu}}PhCH_2$, $^{4\text{-}CF3}PhCH_2$ and $^{3,5\text{-}Me}PhCH_2$) were prepared, in high yields, by reaction of $Mo(CO)_6$ with H_2R_2Cyclam derivatives. The cytotoxic effect of all compounds was examined on human breast cancer cell lines (MCF-7 and MDA-MB-231) and reveals important anticancer activity. Despite complexes displaying a cytotoxic activity comparable to the ligand precursors, they are less active to the non-cancerous human dermal fibroblasts (HDF). In particular, $[(H_2(^{4\text{-}CF3}PhCH_2)_2\text{-}Cyclam)Mo(CO)_3]$ and $[(H_2(^{3,5\text{-}Me}PhCH_2)_2Cyclam)Mo(CO)_3]$ revealed high selectivity against the human breast cancer cell line MCF-7 and deserve further studies as a prospective anticancer drug alternative to the ones in clinical use.

Author contributions

JDGC and LGA: conceptualization; TT, AF, MJF, LCR, FM and LGA: investigation; AF, MJF, LCR, FM, JDGC and LGA: methodology; JDGC and LGA: project administration; FM, JDGC and LGA: supervision; LGA: visualization; LGA: writing – original draft; AF, MJF, FM, JDGC and LGA: writing – review & editing.

Data availability

The data supporting this article have been included as part of the ESI.† Crystallographic data for **5** has been deposited at the Cambridge Crystallographic Data Centre (CCDC) under the deposit number 2301353 and can be obtained from **https://www.ccdc.cam.ac.uk/structures/**.

Conflicts of interest

There are no conflicts to declare.

Acknowledgements

The authors acknowledge Fundação para a Ciência e a Tecnologia, Portugal, for funding within the framework of projects UIDP/00100/2020 (DOI: 10.54499/UIDP/00100/2020), UIDB/00100/2020 (DOI: 10.54499/UIDB/00100/2020), LA/P/0056/2020 (DOI: 10.54499/LA/P/0056/2020) and UID/Multi/04349/2020 (DOI: 10.54499/UIDB/04349/2020).

References

1 H. Sung, J. Ferlay, R. L. Siegel, M. Laversanne and I. Soerjomataram, *Ca-Cancer J. Clin.*, 2021, **71**, 209.
2 F. Bray, M. Laversanne, E. Weiderpass and I. Soerjomataram, *Cancer*, 2021, **127**, 3029.
3 Z. Abbas and S. Rehman, An Overview of Cancer Treatment Modalities, in *Neoplasm*, ed. H. Shahzad, IntechOpen, 2018.
4 T. Makovec, *Radiol. Oncol.*, 2019, **53**, 148.
5 U. Ndagi, N. Mhlongo and M. Soliman, *Drug Des., Dev. Ther.*, 2017, **11**, 599.
6 B. Neuditschko, A. P. King, Z. Huang, L. Janker, A. Bileck, Y. Borutzki, S. C. Marker, C. Gerner, J. J. Wilson and S. M. Meier-Menches, *Angew. Chem., Int. Ed.*, 2022, **61**, e202209136.
7 M. Schutte-Smith, S. C. Marker, J. J. Wilson and H. G. Visser, *Inorg. Chem.*, 2020, **59**, 15888.
8 J. Zhu, A. Ouyang, J. He, J. Xie, S. Banerjee, Q. Zhang and P. Zhang, *Chem. Commun.*, 2022, **58**, 3314.
9 R. Kushwaha, V. Singh, S. Peters, A. K. Yadav, T. Sadhukhan, B. Koch and S. Banerjee, *J. Med. Chem.*, 2024, **67**, 6537.
10 W. M. Motswainyana and P. A. Ajibade, *Adv. Chem.*, 2015, **2015**, 859730.
11 J. F. Machado, M. Machuqueiro, F. Marques, M. P. Robalo, M. F. M. Piedade, M. H. Garcia, J. D. G. Correia and T. S. Morais, *Dalton Trans.*, 2020, **49**, 5974.
12 L. Côrte-Real, F. Mendes, J. Coimbra, T. S. Morais, A. I. Tomaz, A. Valente, M. H. Garcia, I. Santos, M. Bicho and F. Marques, *J. Biol. Inorg. Chem.*, 2014, **19**, 853.
13 T. S. Morais, F. Marques, P. J. A. Madeira, M. P. Robalo and M. H. Garcia, *Pharmaceuticals*, 2022, **15**, 862.
14 I. Ott, *Coord. Chem. Rev.*, 2009, **253**, 1670.
15 J. F. Schlagintweit, C. H. G. Jakob, N. L. Wilke, M. Ahrweiler, C. Frias, J. Frias, M. König, E.-M. H. J. Esslinger, F. Marques, J. F. Machado, R. M. Reich, T. S. Morais, J. D. G. Correia, A. Prokop and F. E. Kühn, *J. Med. Chem.*, 2021, **64**, 15747.
16 G. Moreno-Alcántar, P. Picchetti and A. Casini, *Angew. Chem., Int. Ed.*, 2023, **62**, e202218000.
17 R. Rubbiani, I. Kitanovic, H. Alborzinia, S. Can, A. Kitanovic, L. A. Onambele, M. Stefanopoulou, Y. Geldmacher, W. S. Sheldrick, G. Wolber, A. Prokop, S. Wölfl and I. Ott, *J. Med. Chem.*, 2010, **53**, 8608.
18 S. K. Raju, A. Karunakaran, S. Kumar, P. Sekar, M. Murugesan and M. Karthikeyan, *Ger. J. Pharm. Biomater.*, 2022, **1**, 6.
19 M. Gil-Moles, M. E. Olmos, M. Monge, M. Beltrán-Visiedo, I. Marzo, J. M. López-de-Luzuriaga and M. C. Gimeno, *Chem. – Eur. J.*, 2023, **29**, e202300116.
20 S. Kankala, N. Thota, F. Björkling, M. K. Taylor, R. Vadde and R. Balusu, *Drug Dev. Res.*, 2019, **80**, 188.
21 C. N. Banti and S. K. Hadjikakou, *Metallomics*, 2013, **5**, 569.
22 A. Jurowska, K. Jurowski, J. Szklarzewicz, B. Buszewski, T. Kalenik and W. Piekoszewski, *Curr. Med. Chem.*, 2016, **23**, 3322–3342.
23 X.-M. Luo, H.-J. Wei and S. P. Yang, *J. Natl. Cancer Inst.*, 1983, **71**, 75–80.
24 H. Yanagie, A. Ogata, S. Mitsui, T. Hisa, T. Yamase and M. Eriguchi, *Biomed. Pharmacother.*, 2006, **60**, 349–352.
25 A. V. Konkova, I. V. Savina, D. V. Evtushok, T. N. Pozmogova, M. V. Solomatina, A. R. Nokhova, A. Y. Alekseev, N. V. Kuratieva, I. V. Eltsov, V. V. Yanshole, A. M. Shestopalov, A. A. Ivanov and M. A. Shestopalov, *Molecules*, 2023, **28**, 8079.
26 D. Bandarra, M. Lopes, T. Lopes, J. Almeida, M. S. Saraiva, M. Vasconcellos-Dias, C. D. Nunes, V. Félix, P. Brandão, P. D. Vaz, M. Meireles and M. J. Calhorda, *J. Inorg. Biochem.*, 2010, **104**, 1171–1177.
27 M. S. Saraiva, S. Quintel, F. C. M. Portugal, T. A. Lopes, V. Félix, J. M. F. Nogueira, M. Meireles, M. G. B. Drew and M. J. Calhorda, *J. Organomet. Chem.*, 2008, **693**, 3411–3418.
28 O. Mrózek, L. Melounková, L. Dostál, I. Císařová, A. Eisner, R. Havelek, E. Peterová, J. Honzíček and J. Vinklárek, *Dalton Trans.*, 2019, **48**, 11361–11373.
29 I. Berasaluce, K. Cseh, A. Roller, M. Hejl, P. Heffeter, W. Berger, M. A. Jakupec, W. Kandioller, M. S. Malarek and B. K. Keppler, *Chem. – Eur. J.*, 2019, **26**, 2211–2221.
30 J. Feng, X.-M. Lu, G. Wang, S.-Z. Du and Y.-F. Cheng, *Dalton Trans.*, 2012, **41**, 8697–8702.
31 T. Saravanan and A. Sheela, *ChemistrySelect*, 2024, **9**, e202400618.
32 J. B. Waern, C. T. Dillon and M. M. Harding, *J. Med. Chem.*, 2005, **48**, 2093–2099.
33 J. M. Gretarsdóttir, S. Bobersky, N. Metzler-Nolte and S. G. Suman, *J. Inorg. Biochem.*, 2016, **160**, 166–171.

34 P. M. Abeysinghe and M. M. Harding, *Dalton Trans.*, 2007, 3474–3482.
35 J. Honzíček, J. Vinklárek, M. Erben, Z. Padělková, L. Šebestová and M. Řezáčová, *J. Organomet. Chem.*, 2014, **749**, 387–393.
36 S. Tan, K. Han, Q. Li, L. Tong, Y. Yang, Z. Chen, H. Xie, J. Ding, X. Qian and Y. Xu, *Eur. J. Med. Chem.*, 2014, **85**, 207.
37 J. Y.-C. Chang, G.-L. Lu, R. J. Stevenson, P. J. Brothers, G. R. Clark, K. J. Botting, D. M. Ferry, M. Tercel, W. R. Wilson, W. A. Denny and D. C. Ware, *Inorg. Chem.*, 2013, **52**, 7688.
38 P. B. Cressey, A. Eskandari, P. M. Bruno, C. Lu and M. T. Hemann, *ChemBioChem*, 2016, **17**, 1713.
39 A. J. Gomes, E. M. Espreafico and E. Tfouni, *Mol. Pharmaceutics*, 2013, **10**, 3544.
40 A. Pilon, J. Lorenzo, S. Rodriguez-Calado, P. Adão, A. M. Martins, A. Valente and L. G. Alves, *ChemMedChem*, 2019, **14**, 770.
41 I. Grabchev, S. Yordanova, E. Vasileva-Tonkova, M. Cangiotti, A. Fattori, R. Alexandrova, S. Stoyanov and M. F. Ottaviani, *Dyes Pigm.*, 2016, **129**, 71.
42 C. C. Liolios, C. Zikos, E. Fragogeorgi, D. Benaki, M. Pelecanou, I. Pirmettis, N. Ioannidis, Y. Sanakis, C. P. Raptopoulou, V. Psycharis, A. Terzis, F. Boschetti, M. S. Papadopoulos, G. Sivolapenko and A. D. Varvarigou, *Eur. J. Inorg. Chem.*, 2012, 2877.
43 S. Almada, L. B. Maia, J. C. Waerenborgh, B. J. C. Vieira, N. P. Mira, E. R. Silva, F. Cerqueira, E. Pinto and L. G. Alves, *New J. Chem.*, 2022, 16764.
44 V. Patinec, J.-J. Yaouanc, J.-C. Clement, H. Handel, H. D. Abbayes and M. M. Kubicki, *J. Organomet. Chem.*, 1995, **494**, 215.
45 C.-X. Zhang, D.-W. Fang, J.-L. Wang, A.-Q. Jia and Q.-F. Zhang, *Inorg. Chim. Acta*, 2020, **507**, 119599.
46 R. W. Hay, I. Fraser and G. Ferguson, *J. Chem. Soc., Chem. Commun.*, 1987, 1715.
47 M. Strompor, M. Świtalska and J. Wietrzyk, *Acta Biochim. Pol.*, 2019, **66**, 559.
48 S. D'Errico, A. P. Falanga, D. Capasso, S. D. Gaetano, M. Marzano, M. Terracciano, G. N. Roviello, G. Piccialli, G. Oliviero and N. Borbone, *Pharmaceutics*, 2020, **12**, 627.
49 C. Bézivin, S. Tomasi, F. Lohézic-Le Dévéhat and J. Boustie, *Phytomedicine*, 2003, **10**, 499.
50 E. K. Barefield, *Inorg. Chem.*, 1972, **11**, 2273.
51 L. G. Alves, M. A. Antunes, I. Matos, R. F. Munhá, M. T. Duarte, A. C. Fernandes, M. M. Marques and A. M. Martins, *Inorg. Chim. Acta*, 2010, **363**, 1823.
52 W. T. Dixon, J. Schaefer, M. D. Sefcik, E. O. Stejskal and R. A. McKay, *J. Magn. Reson.*, 1982, **49**, 341.
53 K. Schmidt-Rohr and H. W. Spiess, *Multidimensional Solid-State NMR and Polymers*, Academic Press, London, 1994.
54 *SAINT. Version 7.03A*, Bruker AXS Inc., Madison, WI, USA, 2003.
55 G. M. Sheldrick, *SADABS, Software for Empirical Absorption Corrections*, University of Göttingen, Göttingen, Germany, 1996.
56 A. Altomare, M. C. Burla, M. Camalli, G. L. Cascarano, C. Giacovazzo, A. Guagliardi, A. G. G. Moliterni, G. Polidori and R. Spagna, *J. Appl. Crystallogr.*, 1999, **32**, 115.
57 G. M. Sheldrick, *Acta Crystallogr.*, 2015, **C71**, 3.
58 L. J. Farrugia, *J. Appl. Crystallogr.*, 2012, **45**, 849.
59 C. F. Macrae, I. Sovago, S. J. Cottrell, P. T. A. Galek, P. McCabe, E. Pidcock, M. Platings, G. P. Shields, J. S. Stevens, M. Towler and P. A. Wood, *J. Appl. Crystallogr.*, 2020, **53**, 226.

